TÜBİTAK

Turk J Phys
33 (2009) , 139 – 148.
© TÜBİTAK
doi:10.3906/fiz-0811-8

Transport property measurements of Bi_2Se_3 crystal grown by Bridgman method

M. P. DESHPANDE, Nilesh N. PANDYA, and M. N. PARMAR
Department of Physics, Sardar Patel University, Vallabh Vidyanagar
388120, Gujarat, INDIA
e-mail: vishwadeshpande@yahoo.co.in

Received 14.11.2008

Abstract

This paper deals with the growth of Bi_2Se_3 crystal by newly designed experimental set-up of Bridgman technique in our laboratory. Grown crystal is characterized by EDAX (Energy Dispersive Analysis of X-rays), XRD (X-ray Diffraction), low temperature thermopower measurements (17–284 K), resistivity measurements (16–294 K) and Hall Effect at room temperature in order to study its various properties. The surface study of the grown crystal using AFM (Atomic Force Microscopy) shows a hexagonal unit cell shape whose internal angle determined comes out to be nearly equal to 122.94° which has close resemblance with an angle of 120° of perfect internal angle of hexagon. Various parameters obtained from above measurements like lattice parameters, crystallite size and stacking fault probabilities are discussed in detail in the paper.

Key Words: Crystal growth, transport properties, thermoelectric materials, atomic force microscopy.
PACS: 72.15.Eb; 72.15.Jf

1. Introduction

Bi_2Se_3 is a narrow band gap material crystallizing in hexagonal structure [1]. Bi_2Se_3 has useful application in the field of thermoelectric devices as solid state coolers or generators [2–5] therefore studies on various properties of Bi_2Se_3 are interesting for both basic and applied research. Even though bismuth selenide is not as technologically important as bismuth telluride, Bi_2Se_3 is properly crystallizable under controlled conditions and easily cleavable. Hence it could be considered a model compound among thermoelectric materials for both experimental and theoretical analysis.

2. Experimental

The basic process of crystal growth by Bridgman method is mentioned by Brice [6]. We have designed in our laboratory an experimental set up which implements a slight modification in this technique and is used for the growth of Bi_2Se_3 crystal.

Modifications made in the Bridgman set up are: (a) Use of 900 rpm motor with gear box, instead of a stepper motor; (b) Use of threaded shaft and threaded screw, instead of a pulley mechanism for lowering of sample; (c) Use of flip-flop timer circuit for controlling the lowering rate.

Advantages of the modified set up are: (a) Accurate displacement of ampoule; (b) The elastic impact of temperature on sample holder wire is nullified by keeping its length short; (c) The problem of jerks along the linear motion is nullified here; (d) New design of set up is of low cost.

The quartz ampoule containing Bi_2Se_3 material is sealed at 10^{-5} torr and placed in a vertical high temperature furnace at a temperature of 715 $^\circ$C (tip of the ampoule). The lowering rate of this ampoule is kept at 0.5 mm/hr. A crystal grown by this technique and cleaved portions are shown in Figure 1.

The stoichiometry of the grown crystal is confirmed by EDAX. Further, characterization is done by X-ray diffraction in order to calculate lattice parameters, crystallite size and stacking fault probabilities of this sample. As the material is thermoelectric in nature, we measured the thermopower in the temperature range 17 K to 284 K and Vander Pauw resistivity in the temperature range 16 K to 294 K with existing facilities available at IUC-DAE Indore. Hall effect measurements were done at room temperature on this sample via a Lakeshore 7504 Hall measurement system in our department. To gain insight into the surface of the cleaved crystals, analysis using a atomic force microscope was also carried out.

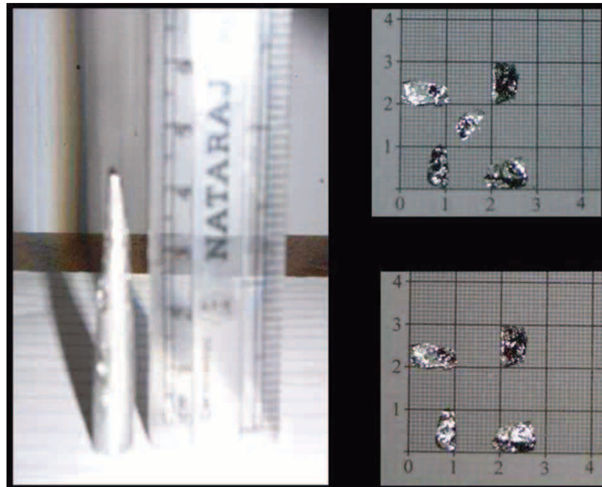

Figure 1. Photograph of as-grown and cleaved crystal of Bi_2Se_3.

3. Results and discussion

3.1. Energy Dispersive Analysis of X-rays

The EDAX spectra shown in Figure 2 of the sample shows that the grown crystal is free from any other impurities; and Table 1 provides the mass fraction of each element, i.e. bismuth and selenium, used during the growth as well that measured via EDAX. This indicates the stoichiometry in the crystal is well maintained.

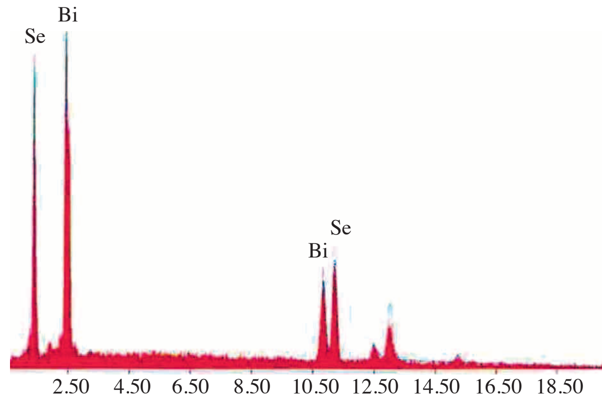

Figure 2. EDAX spectra of Bi_2Se_3 crystal.

Table 1. Results obtained from EDAX.

Element	Growth as mixed, wt%	EDAX, wt%
Bi	63.80	61.73
Se	36.20	38.27

3.2. X-ray diffraction

X-ray diffractogram of powder Bi_2Se_3 was obtained using a Philips X-ray diffractometer and is shown in Figure 3. The values of lattice parameters, X-ray density and volume, are calculated for this sample and shown in Table 2; the values have close resemblance with reported values. Calculations of crystallite size were carried out using the Scherrer formula [7]:

$$t = \frac{k\lambda}{\beta_{2\theta}\cos\theta}, \tag{1}$$

where k is constant having value 0.9, λ is the wavelength of the X-ray source, $\beta_{2\theta}$ is the FWHM (full width at half maximum) line width of the intensity lines. Calculated crystallite size shows variation from 116 Å to 695 Å for different reflections taken into consideration.

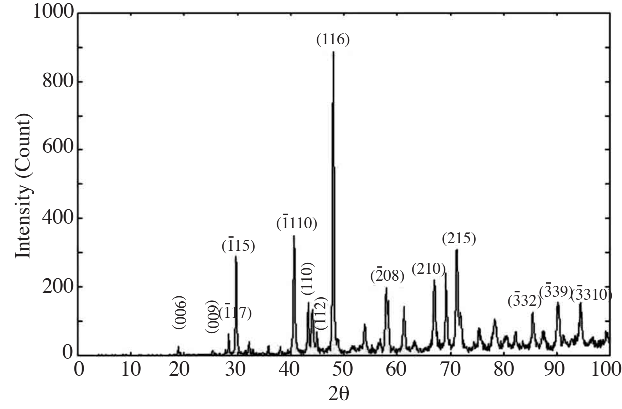

Figure 3. X-ray diffractogram of Bi_2Se_3 compound.

Table 2. Lattice Parameters, unit cell volume and X-ray density obtained from X-ray diffractogram of Bi_2Se_3 sample.

Parameter	Bi_2Se_3	
	Reported [8]	Calculated
a (Å)	4.13	4.12
c (Å)	28.62	28.63
c/a ratio	6.92	6.94
Volume V=($\sqrt{3}/2$)a^{2}c Å^3	425.14	422.18
X-ray density (gm/cc)	7.676	7.720

Warren and Agarwal et al. [9, 10] has shown that, in the case of hexagonal closed-packed structure, it is possible to make a realistic estimation of both the deformation fault probabilities α and growth fault probability β by measuring the half width of the X-ray diffraction lines using the following expression:

$$\text{For even} l : (3\alpha + 3\beta) = \frac{B_{2\theta}\pi^2 c^2}{360\ l\ d^2 \tan\theta} \quad (2)$$

$$\text{For odd} l : (3\alpha + \beta) = \frac{B_{2\theta}\pi^2 c^2}{360\ l\ d^2 \tan\theta}, \quad (3)$$

where $B_{2\theta}$ is the full line width, expressed in degrees, at half the maximum intensity, $c = 2d_{002}$, l is a Miller index, d is the interplanar spacing for the reflection, α is deformation fault probability and β is the growth fault probability.

Deformation fault probability α and growth fault probability β, calculated from the above equations, are shown in Table 3, and the values indicate that there may be a deformation fault probability of 23 per 1000 atomic layers, and growth fault probability of 10 per 1000 atomic layers for Bi_2Se_3 samples.

Table 3. Deformation fault probability α and growth fault probability β for Bi_2Se_3 crystal.

Reflections	$(\bar{3}38),(\bar{3}39)$
$\beta_{2\theta}$ (Degree)	0.24, 0.36
$3\alpha+3\beta$	0.06
$3\alpha+\beta$	0.08
α	0.023
β	0.010

The values of α shown in Table 3 clearly indicate that a high density of deformation faults were introduced into the specimen and the actual number depended upon the amount of deformation introduced into the sample during experiment. In the case of growth fault probability, a firm conclusion is difficult in view of small values of β. But, it is presumed that stacking faults may be responsible for the conductivity phenomena in this sample.

3.3. Low temperature Thermoelectric Power (TEP) measurement

As Bi_2Se_3 is known to be a good thermoelectric material, it is essential to measure its thermoelectric power S in order to calculate its figure of merit. Hence, Figure 4 shows the variation of Seebeck coefficient with an inverse of temperature for Bi_2Se_3 crystal in the temperature range 16 K to 200 K.

A study from Figure 4 reveals that in all the cases, the absolute value of S increases steadily with an increase in temperature, for Bi_2Se_3 sample, such increase of S at lower temperature is due to the decrease of electron mobility with temperature [11, 12]. Secondly the sign of TEP depends on whether the majority carriers are electrons or holes. The fact that TEP in Bi_2Se_3 crystal is negative clearly indicates that this crystal is n-type in nature.

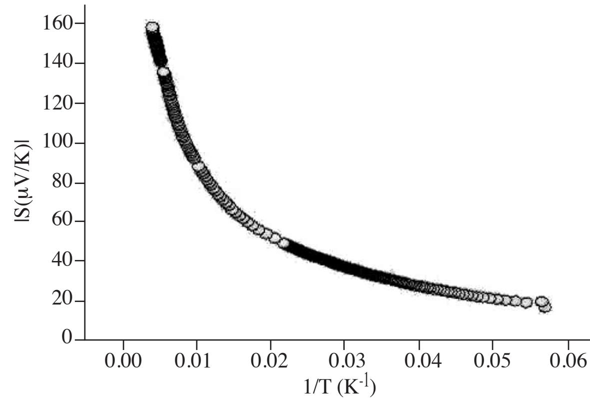

Figure 4. Plot of thermoelectric power S as a function of inverse of temperature for Bi_2Se_3 crystal.

3.4. Low temperature resistivity measurements

The set-up to conduct resistivity measurement is similar to that used for Seebeck coefficient measurement except the way contacts were established on the sample. In the present Seebeck measurement, we use two copper block sample holders and the sample is placed in between these two blocks; in case of resistivity measurement,

four contacts were made onto the sample with copper wires and current was allowed to pass through two outer contacts and voltage is measured between the two inner contacts.

Figure 5 shows how Bi_2Se_3 crystal resistivity varies in the temperature range 16–294 K. The peculiar result, seen in Figure 5, is that resistivity goes on increasing with temperature, i.e. electrical conductivity monotonically decreases with temperature and matches with the result observed by [11–19].

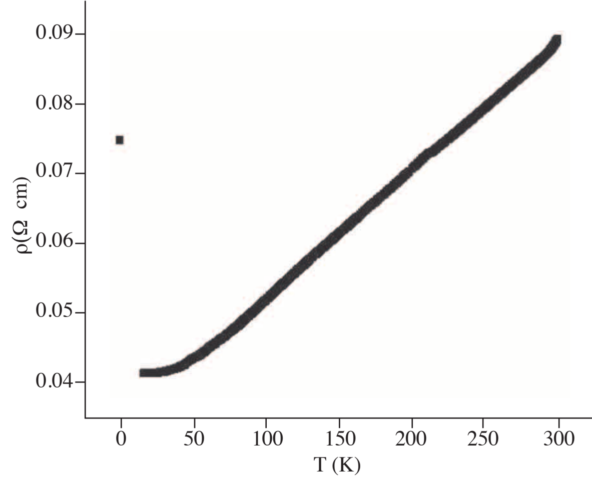

Figure 5. Plot of resistivity ρ as function of temperature T in Bi_2Se_3 crystal.

As explained in [12], for values measured above 300 K, resistivity decreases with increase in temperature. However, high temperature resistivity measurements were not possible due to the experimental setup in this investigation. It is clear such crystals can exhibit semimetallic conduction up to 300 K above which they can show semiconducting behavior, and from where we can obtain the transition temperature. The semimetallic character arises in Bi_2Se_3 due to the half filled 6p band overlapping the filled 6s band. It is also stated [12] the presence of interstitial defects may result in ionized states with rise in temperature and provide free electrons for the conduction mechanism, thereby decreasing the absolute value of the electrical resistivity.

In [11] is reported that, in low temperature portion of the resistivity measurements, semiconducting behavior can be observed based on the purity of material used. In our case, increase of electrical resistivity with temperature in the low temperature region can be attributed to the temperature dependence of carrier mobility [18].

3.5. Hall Effect Measurements

In order to support the present results, Hall effect measurements on Bi_2Se_3 crystal has been carried out at room temperature using a Lakeshore 7504 Hall measurement system [20]. The measurements were carried out by passing a 100 μA current through the sample under magnetic fields +5 kG to -5 kG; data is shown in Table 4. The results obtained show that all the Hall coefficients, R_H, are negative, which means that our sample is n-type in nature thereby supporting the Seebeck coefficient measurements. Values of R_H obtained varies from -1.6 to -3.3 cm^3/C and are somewhat higher than reported [12, 21]; mobility μ_H varies from 4.68×10^2 to 1.15×10^3, which are also higher than reported [22]; and carrier density n varies from 0.5×10^{18} to 3.6×10^{18}

cm^{-3}, which is one power lower than the reported values [12, 22, 23]. The measured zero field resistivity comes out to be 86 mΩ. cm; whereas the reported values are 3 to 4 mΩ. cm.

Table 4. Values of Hall coefficient R_H, mobility $\mu_{\rm H}$, carrier concentration n of Bi_2Se_3 crystal. Current = 100 μA; Zero field Resistivity = $8.623\times 10^{-2}\Omega$. cm.

B (kG)	Hall coefficient, R_H (cm^3/C)	Hall Mobility, $\mu_{\rm H}$ (cm^2/Vs)	Density, n (cm^{-3})
+5	−2.246	6.2×10^2	2.7×10^{18}
+4	−4.177	1.1×10^3	1.4×10^{18}
+3	−3.065	8.4×10^2	2.0×10^{18}
+2	−1.697	4.6×10^2	3.6×10^{18}
+1	−3.365	9.2×10^2	1.8×10^{18}
−1	−11.39	3.1×10^3	5.4×10^{17}
−2	−2.357	6.5×10^2	2.6×10^{18}
−3	−3.898	1.0×10^3	1.6×10^{18}
−4	−4.317	1.1×10^3	1.4×10^{18}
−5	−2.547	7.0×10^2	2.4×10^{18}

3.6. Atomic Force Microscopy (AFM) surface studies

The as-grown crystal of Bi_2Se_3 was viewed under contact mode with a Veeco AFM and a silicon nitride tip was used to obtain a topographic image of the sample surface. The Fourier transform images obtained with the help of the Nanoscope Controller software for Veeco scanning force microscopes is displayed in Figure 6; the images show 2-D and 3-D topographic images of the crystal surface thereby confirming the regular (periodic) arrangement of atoms throughout the (5.547 nm square) scanned region of the sample.

Figure 7 shows the section analysis for the periodicity exhibited in Figure 6. The analysis makes clear the atomic arrangement is periodic. The inset values shows the horizontal distance between two successive atoms and are nearly equal to 4.14 Å on both a and b axes. Figure 8 shows the section analysis for angle, of Fourier transform image of Figure 6 representing a hexagonal unit cell shape whose angle determined comes out to be nearly equal to 122.94° and has close resemblance to the 120° of a perfect hexagon.

Bi_2Se_3 crystal has been grown successfully in our laboratory using the modified Bridgman technique. Seebeck co-efficient and Hall effect measurements indicates that the sample is n-type conductive in nature. The increase in resistivity from low temperature to 300 K is attributed to the semi-metallic behavior of this crystal. Atomic Force Microscope images reveals the regular arrangements of atoms in the 5.547 nm scanned region and also provides a measure of the hexagonal unit cell angle which nearly equals to 122.94°.

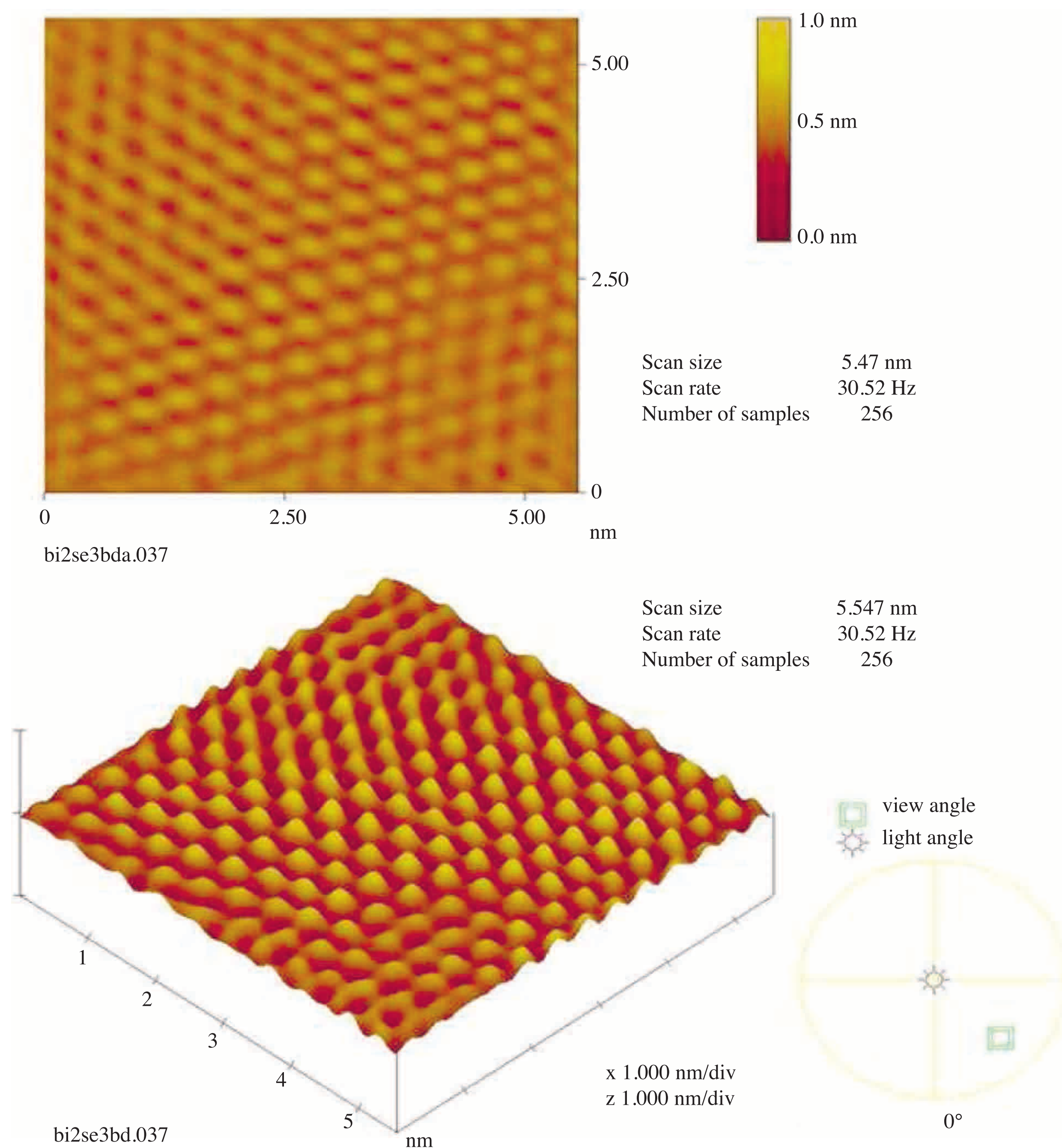

Figure 6. 2-D, 3-D Fourier transform images of Bi_2Se_3 crystal.

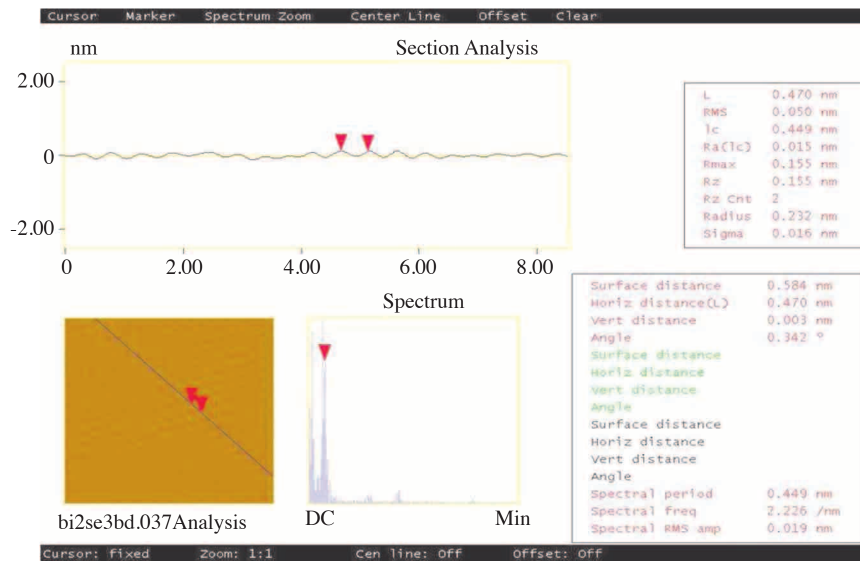

Figure 7. Section analysis (periodicity) of Fourier transform image taken at atomic scale.

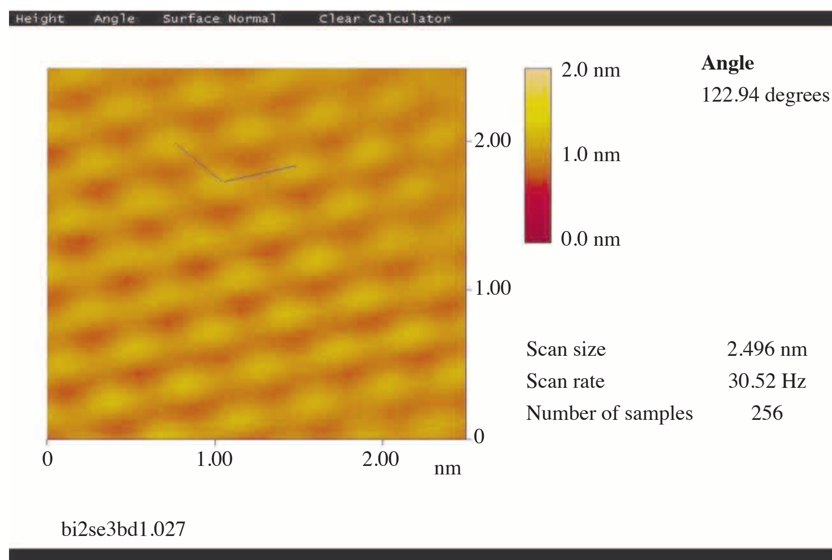

Figure 8. Section analysis (angle) showing internal angle of hexagonal unit cell.

Acknowledgements

Authors are thankful to UGC for providing DRS/SAP (IIIrd phase) programme to the Department of Physics, Sardar Patel University, which has made this work possible. Thanks are specifically directed to Dr. V. Ganesan, Miss Swati Pandya and other students of the low temperature laboratory IUC-DAE, Indore for helping round the clock to carry out TEP, Low temperature resistivity and AFM work.

References

[1] S. Augustine and E. Mathai, *Mater. Res. Bull.*, **36**, (2001), 2251.

[2] U. Birkholz, *Amorphe und Polykristalline Halblein* (Springer, Berlin, 1984).

[3] H. J. Goldsmid, *Thermoelectric Refrigeration* (Plenum, New York, 1964).

[4] A. F. Yoffe, *Semiconductor Thermoelectric Cooling* (London, 1957).

[5] D. M. Rowe, *CRC Handbook of thermoelectrics* (Chemical rubber, Boca Raton, FL.1995)

[6] J. C. Brice, *The growth of crystals from liquids*, (North Holland, 1973).

[7] B. D. Cullity, *Elements of X-ray Diffraction (2nd Edition),* (Addison-Wesley, 1978) p.102.

[8] P. Quing, D. Yajie, D. Zhaoxing, L. Yadong, *Inorg. Chem.,* **41**, (2002), 5249.

[9] B. E. Warren, *Progr. Met. Phys.*, **8**, (1959), 147.

[10] M. K. Agarwal and M. J. Capers, *J. Appl. Cryst.*, **9**, (1976), 4007.

[11] D. B. Hyun, J. S. Hwang, B. C. You, *J. Mater. Sci.,* **33**, (1998), 5595.

[12] S. Augustine et al., *J. Phys.: Condens. Matter*, **17**, (2005), 2873.

[13] K. Seeger, *Semiconductor Physics* (Springer-Verlag, New York, 1986).

[14] K. Jacob John, B. Pradeep and E. Mathai, *Solid State Commun.*, **85**, (1993), 879.

[15] T. Caillat, A. Borshchecsky, J. P. Fleurial, *J. Appl. Phys.*, **80**,(1996), 4442.

[16] D. Mandrus, A. Migliori, E. J. Peterson and J. D. Thompson, *Phys. Rev. B,* **52**, (1995), 4926.

[17] D. T. Morell, G. P. Meisner, *J.Appl.Phys.*, **77**, (1995), 3777.

[18] J. W. Sharp, E. C. Jones, R. K. Williams, P. M. Martin and B. C. Sales, *J.Appl.Phy.,* **78**, (1995), 1013.

[19] E. Koukharenko, N. Frety, V. G. Shepelevich, J. C. Tedenac, *J. Alloys Compd.*, **299**, (2000), 254.

[20] User's Manual-Lakeshore 7500/9500 series Hall System, Vol.1, Lakeshore Cysotronics, Inc. (1999)

[21] P. Lostak, C. Drasar, H. Sussmann, P. Reinshaus, L. Benes, *J. Cryst. Growth*, **179**, (1997), 144.

[22] V. F. Boechko, *Inorg. Mater.* (USA), **11**, (1975), 1288.

[23] S. Urazhdin, D. Bilc, S. D. Mahanti, S. H. Tessmer, *Phys. Rev. B*, **69**, (2004), 085313.